Journal of Chemical Engineering & Process Technology

Luo S, et al., J Chem Eng Process Technol 2018, 9:4
DOI: 10.4172/2157-7048.1000392

Research Article Open Access

A Continuous Directional Solvent Extraction Desalination Process Realized with the Aid of Electro-coalescence

Shirui Luo[1], **Yunsong Pang**[1] **and Tengfei Luo**[1,2*]

[1]*Department of Aerospace and Mechanical Engineering, University of Notre Dame, Notre Dame, IN 46556, USA*

[2]*Center for Sustainable Energy at Notre Dame (ND Energy), University of Notre Dame, Notre Dame, IN 46556, USA*

***Corresponding author:** Tengfei Luo, Department of Aerospace and Mechanical Engineering, University of Notre Dame, Notre Dame, IN 46556, USA, Tel: +574-631-9683; E-mail: tluo@nd.edu

Received date: November 19, 2018; **Accepted date:** November 27, 2018; **Published date:** November 30, 2018

Abstract

The recently demonstrated non-membrane, low-temperature directional solvent extraction (DSE) is promising to reduce desalination cost by eliminating the need of membranes and utilizing low-temperature energy sources from solar energy or waste heat. This paper investigates the technical feasibility of a continuous DSE water desalination process using decanoic and octanoic acid as directional solvents (DS). A continuous lab-scale DSE prototype is realized with the aid of electro-coalescence (EC) with a capacity of producing 28 ml/h of freshwater. A preliminary economic analysis shows that the operational cost of DSE desalination is estimated to be ~$3.03/m^3. Our results reveal two critical technological aspects that need further research to push DSE closer to deployment. These include (1) identifying more effective DSs with higher water yield; (2) optimizing the EC to improve the separation efficiency and effectiveness. Both aspects will be critical to increase water production rate and decrease energy cost of DSE desalination. Our cost analysis indicates that the desalination cost of DSE can reach ~$0.25/m^3, if the DS performance can be improved by four-folds and the EC efficiency is increased to 90%. In summary, the current work lays a framework upon which further research on the continuous DSE desalination process can be based. Once it is mature and widely deployed, DSE is promising to lower the desalination cost by utilizing low-temperature waste heat, which will contribute significantly to ameliorating the global water scarcity problem.

Keywords: Desalination; Waste heat; Directional solvent extraction; Electro-coalescence

Introduction

Water scarcity already affects every continent, and it is among the most serious challenges faced by the world. Almost one-fifth of the Earth's population is living in regions of physical water scarcity such as the Middle East, North Africa, and South Asia, and 1.6 billion people are facing economic water shortage in developing countries where accessing and transporting water from fresh aquifers is expensive [1]. While solving the water scarcity problem is multifaceted, including aspects such as better water management and wastewater reuse, desalination is the only method that actually increases the water supply beyond what is available from existing freshwater resources [2]. However, less than 1% of the global freshwater supply was from desalination by Nikolay [3], primarily because desalination processes of all types are high-cost [4] and energy-intensive [5], making the product generally about 3-6 times more expensive than water from existing sources. Moreover, the energy used for existing desalination technologies is mainly from nonrenewable fossil fuels whose use leads to greenhouse gases emissions and results in environmental problems. Desalination cost may likely increase over time as the world's fresh-water and fossil-fuel supplies both dwindle. Though the U.S. National Research Council roadmap for water desalination sets a target of 50-80% reduction in desalination costs by 2020, this may not be achievable by incremental improvements in current technologies alone [5].

Current major desalination technologies can generally be divided into two kinds: thermal distillation and membrane-based processes [6,7]. Widely used thermal distillation desalination includes multi-stage flash distillation (MSF), multiple-effect distillation (MED) and vapor compression, and these total one-half of the global desalination installed capacity. One significant problem with distillation techniques is the consumption of high temperature (70-120°C) thermal energy since distillation desalination must overcome the latent heat requirement [8]. The biggest competitor of distillation desalination processes is the membrane-based reverse osmosis (RO) process, which accounts for 44% of the global desalinated water production [9]. This process is popular since it uses less energy than distillation and therefore results in a lower overall desalination cost. However, this gain is obtained by applying very high pressures (5-8 MPa) which require the consumption of significant electrical energy. Membranes, which are essential in RO plants, can have fouling problems and need routine maintenance and replacement every few years [10]. This leads to increased capital and maintenance cost of the RO plants.

Besides the two major technologies, the solar heating-induced steam generation by combining heat localization and thin-film evaporation is gaining its popularity recently in distillation water desalination and sanitization [8,11-13]. The water vapor can be generated despite the bulk temperature lower than the boiling point, due to highly efficient localized surface plasmon resonance effect for gold nanoparticles [14] or thin-film water evaporation for graphene [8,11]. However, this method is restricted to harvest only the solar thermal energy rather than waste heat.

As demonstrated in the above review of the current state-of-the-art in water desalination, major challenges that can be singled out are

related to energy consumption and the reliance on membranes. Energy consumption contributes a large portion of the cost in both MSF (50%) and RO (44%) processes, while membrane replacement in the RO desalination contributes 7-12% to the overall desalination costs [15]. These technologies are expected to remain energy intensive, and future costs may strongly depend on the price of fossil fuels which is likely to increase [16]. Reliance on fossil fuels can also lead to environmental issues. Another challenge is that the sizes of distillation plants cannot be scaled down, and the desalination costs of small-scale RO plants are high [17]. These methods are currently most suitable for centralized, large-scale desalination to be cost-effective. Development of novel, inexpensive desalination processes that do not directly rely on fossil fuels is thus imperative.

Recently, a non-membrane, low-temperature directional solvent extraction (DSE) desalination process has been demonstrated by Bajpayee [18-20] which has the potential to reduce desalination cost by eliminating the need of membranes and utilizing very low-temperature energy sources that are readily available from solar energy, geothermal energy, or waste heat. With a very low top brine temperature of 40-50°C, this desalination process was predicted to consume less exergy compared to both RO and MSF [18]. The DSE process uses a special solvent called directional solvent (DS). The key to this process is the directionality of the solvent, meaning it should have the ability of dissolving water while rejecting salt and itself being insoluble in water. This solvent has the following features: (1) The solvent can dissolve water; (2) The water solubility increases with temperature; (3) The solvent is insoluble in water; and (4) The solvent does not dissolve salt ions. Theoretical studies and batch experiments have been performed previously [18,20-22], but a truly continuous loop that can closely mimic a real desalination plant has not been demonstrated. The bottleneck and speed-limiting step of accomplishing the continuous DSE desalination was determined to be the water-DS phase-separation process [23]. Bajpayee tried an in-line centrifuge to build a semi-continuous loop to assist the phase separation [23]. However, the centrifuge was very energy intensive and not feasible for real industrial application. He also reported that the in-line centrifuge did not perform well in separating the water-in-DS micro-emulsion even with flow rates as low as 0.01 L/s. He placed the collected emulsions in conical tubes and centrifuged in a laboratory centrifuge as an alternative. As such, to take the DSE concept closer to field application, a truly continuous process that can overcome the phase separation bottleneck in an energy-effective manner needs to be studied and demonstrated.

This study presents a lab-scale continuous DSE loop with the capacity of producing 28 ml/h of freshwater with a salinity <500 ppm-the drinking water standard. To overcome the phase separation limitation, the electric field-assisted phase separation, Electro-coalescence (EC), is implemented to enable the continuous loop. EC is one of the most common separation processes in refineries, petroleum, food and water-treatment industry, because it is environmentally friendly and energy-efficient [24]. The continuous loop is demonstrated to eliminate all the manual procedures involved in a batch process and reduce the cycle time by expediting the separation process. A preliminary economic analysis is also performed based on the operation data from the loop with EC. Our study indicates that since DSE desalination has no demand for high-grade energy input, it can be very competitive in cost where low-temperature heat, such as solar thermal energy, geothermal, and waste heat, is abundant. Our results also reveal two critical technological aspects that need further research to push DSE closer to deployment. These include (1) identifying more effective DSs with higher water yield; (2) optimizing the EC to improve the separation efficiency and effectiveness. Both aspects will be critical to increase water production rate and decrease energy cost of continuous DSE desalination.

Experimental Setup

The DSE technology uses DS going through a cyclic process that consists of forming a saline water-in-solvent emulsion, heating the emulsion so that pure water is dissolved into the solvent, removing the brine-phase, and cooling the solvent to precipitate out pure water. A schematic diagram of the continuous desalination loop consists the following steps is depicted in Figure 1. Feed saline water enters the system and mixes with the DS in the hot tank. During heating in the hot tank, a certain amount of water molecules diffuse into the DS due to the higher solubility at higher temperatures. Due to the directional feature of the solvent, salt ions do not dissolve into the DA but stay in the water phase to form concentrated brine. The brine is drained out of the loop.

- The stream exits the hot tank and enters another gravitational separator to settle down the suspended water droplet to ensure that the outlet stream only contains DS and water.
- The hot DS-water solution is then cooled down. After cooling, the DS-water solution becomes supersaturated due to the solubility decrease with lowering temperature, water molecules will precipitate out as suspended micro-size water droplets to form water-in-DS emulsion.
- The separation process of the water-in-DS emulsion is the rate-limiting step, which is significantly enhanced by our home-designed electrocoalescer. It involves several concomitant electrohydrodynamic phenomena wherein an electric field is used to assist the merging of small water droplets dispersed in a continuous oil phase.
- After phase separation, the freshwater at the bottom of the two phase is then extracted. The DS phase at the top is pumped back to the hot tank again to start another cycle.

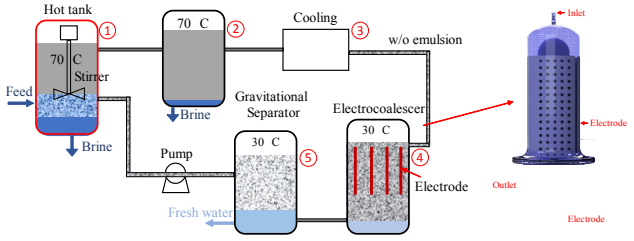

Figure 1: Schematic diagram of the lab-scale continuous DSE loop (left); Schematic diagram of the custom-built in-line electrocoalescer (right).

The adapted binary liquid phase diagram with asymmetric solubilities and no critical point is provided to better demonstrate the phase change process of weakly miscible DS/water mixture in step 1-3 in Figure 1. The ϕ means a status of pure DS-water solution when a small amount of water is fully dissolved in solvent, the solvent is undersaturated, similarly the η means pure DS-water solution when a small amount of solvent is fully dissolved in water. The ϕ+η means that the solvent and water is not fully dissolved in each other. There are extra water or solvent that not dissolved. The yellow plot represents

solvent cycle and the blue plot represents water cycle. In a generic solvent cycle, the mixture is heated and saturated from point 1 to point 2, this is called as temperature dependent solubility (Figure 2). Then the saturated solution is cooled from point 2 to point 3 to be supersaturated. The precipitation process is from point 3 to point 1. The phase diagram of an ideal directional solvent that suitable for DSE desalination is presented in Figure 2b. The solvent ideally has high temperature dependent solubility to yield more water production. The solvent also has a sharp increase in water solubility and low solubility dissolved at cold temperature to reduce the solvent loss.

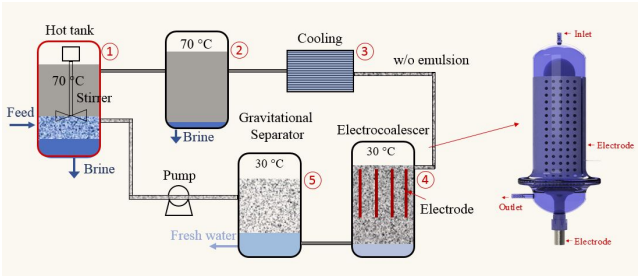

Figure 2: Generic cycle for solvent with directional property (left); Ideal cycle when solvent has sharp increase in water solubility and low water solubility at cold temperature, which will eliminate the water cycle (right).

The dissolution and precipitation process can also be explained from a microscopic point of view. Octanoic acid (OA) and decanoic acid (DA) are used as an example for DS. During the heating, the hydrogen bonds among OA chains are broken, causing the oxygen atom in the carboxyl group of OAs to be available for water molecules to bind on. After sufficient time, the OA is saturated with water molecules. The saturated solution is quenched at different cooling rates to reach ambient temperature. Since the solubility of water in OA decreases with temperature decrease, the excess dissolved water molecules in the supersaturated solution will detach from the OA and precipitate out to form micro-droplets, forming a stable water-in-oil emulsion. Figure 3 illustrates the precipitation process at the molecular level after cooling. Initially in the saturated water/oil solution, the water and OA molecules are stably bonded by hydrogen interactions. Then after cooling, the hydrogen bonds among carboxyl groups in OA and water molecules are detached due to supersaturation. The detached water molecules will finally congregate to form dispersed water droplets.

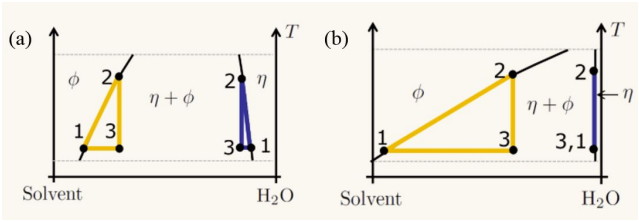

Figure 3: Precipitation of micro-size droplet in water-in-oil emulsion from a microscopic point of view.

The speed-limiting step in the DSE process is the phase separation of the water-in-oil micro-emulsion (step 4 in Figure 1). This is because the thermodynamically unstable water-in-DS emulsion was produced after the cooling process (step 3). During the supersaturation, the dissolved water molecules precipitate out to form small droplets with sizes typically ranging from 1 to 20 μm. These small water droplets lead to very large water/DS interfaces and low sedimentation rates, making the separation a speed limiting step of the whole continuous loop. Phase separation of water-in-oil emulsions is one of the most common processes in the chemical and petroleum industry. While the accumulated literature is vast and the techniques are multifarious, phase separation is generally accomplished via two distinct strategies: (1) mechanical and (2) interfacial chemistry modification. The mechanical approach (usually centrifugation) of phase separation involves the application of centrifugal force to separate according to their difference density or viscosity of the medium. This method suffers from low efficiencies and high energy consumption when employed to a large volume of emulsion. The modification of interfacial chemistry usually requires the use of surfactants, which are expensive and need extra steps to be eliminated from the final products. Because it is environmentally friendly and energy-efficient, EC has found wide industrial application as an effective de-emulsification method [24,25]. For instance, many petroleum refining processes utilize electrostatic fields to dehydrate water-in-oil emulsions [26]. EC can be implemented to prompt the separation of salt-free production water from the directional solvent and thus make DSE an efficient process. To facilitate the separation of the emulsion, a non-intrusive electrostatic separation system was incorporated into our DSE loop. This EC can assist the merging of small droplets into larger ones due to combined electrohydrodynamic effects discussed elsewhere [24,27] which significantly speed up the separation process. The film drains radially outwards under the electrostatic force until it reaches to a cutoff thickness that allows the rupture of droplets interface. The merging and coalescence of adjacent small droplets promoted by an electric field will increase droplet size and eventually break the quasi-equilibrium of the emulsion, leading to phase separation. Figure 1 (right) illustrates a schematic diagram of the designed electropolished. A vertical arrangement of two concentric cylinders is adopted in our design. There are two reasons for employing this geometry: (a) a non-uniform field from the cylindrical electrodes can enhance the performance of EC compared to a uniform field, due to the combined effect from the dipole-dipole interaction and dielectrophoretic [27]; and (b) due to gravity, vertically arranged electrodes could prevent big droplets from aggregating on the surface of the electrodes to largely avoid short-circuiting the electrodes.

Results and Discussion

Continuous loop test

The whole system was constructed inside a fume hood. Two different DSs were tested, including octanoic acid (OA) and decanoic acid (DA). The OA and DA are important ingredients in many dairy products.

Phase	Density (kg/m^3)	Dielectric constant	Viscosity (cp)	Electrical Conductivity (S/m)
Deionized water	997	80	0.9	5.5×10^{-6}
OA	907	2.5	5.748	$<10^{-8}$
DA	893	2.3	4.327	$<10^{-8}$

Table 1: Physical properties of the water-in-oil emulsion at T=25°C.

For example, decanoic acid exists in whole milk with a concentration of 1300 ppm (parts per million) [28]. These fatty acids were reported to be suitable DSs, and the chemical properties such as temperature-dependent solubilities, ion rejection rates, viscosities and electrical conductivities can be found in previous papers [18,20,29]. For example, the fitted relative solubility of water in OA at different temperatures shows a good linear solubility dependency on temperature with slope 0.07%/°C, meaning 10 degree increase in temperature will yield 0.7 wt% increase in solubility [29]. Other physical properties of water and OA are given in Table 1.

To mimic seawater composition as the feed water, a combination of four salts, NaCl, KCl, $CaCl_2$ and $MgSO_4.6H_2O$, was dissolved in deionized water. The combination contains 2.740 g NaCl, 0.076 g KCl, 0.370 g $CaCl_2$, and 0.645 g $MgSO_4{\cdot}6H_2O$ in 100 g solution with deionized water. This matches the concentrations of Na^+ (1.80% w/w), Cl^- (1.93% w/w), K^+ (0.04% w/w), and SO_4^{2-} (0.27% w/w) ions found in typical seawater. To demonstrate the effective operation of the DSE prototype, experiments were run continuously with the prototype under different test conditions, including different operating temperatures and two different flow rates (1.17 and 1.50 ml/s). The freshwater yield from the loop as a function of temperature differences (ΔT) and flow rate was obtained. Freshwater yield is defined as the ratio of the freshwater flow rate to the DS flow rate. ΔT is defined as the difference between the highest and the lowest temperatures in the cyclic process.

The results of freshwater yield using OA as the DS under different temperatures are summarized and presented in Figure 4. A close to linear relationship between the yield and the operating temperature difference is obtained from the continuous loop. This trend is similar to that found from the batch processes [20], which achieved complete phase separation using centrifuge instead of using EC in the continuous loop. However, the absolute water yield at each temperature difference was smaller compared to that from the batch process. Under a certain ΔT, the freshwater yield from the continuous prototype is ~30% of that from the batch process.

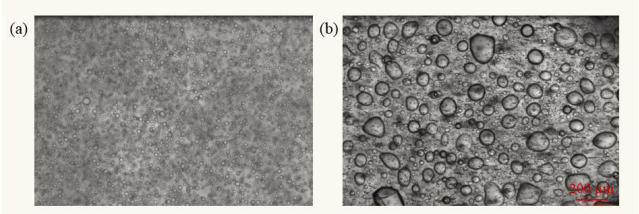

Figure 4: Precipitation of micro-size droplet in water-in-oil emulsion from a microscopic point of view.

The DSE prototype was also tested using DA as the DS. DA has similar properties to OA since both are fatty acids. The slightly longer carbon chain enables DA to have smaller residue in produced water (35 ppm) [20] compared to OA (680 ppm) [30]. However, DA has a melting point of 32°C and will solidify easily under room temperature. Solidification at any location of the loop will cause the deactivation of the loop, since the pressure balance will be broken, and the water/DA fluid will be stagnant. To avoid solidification, we wrapped every component and pipe with heating tape and covered them with thermal insulating material to maintain the fluid in the liquid phase and prevent blockage. Here, we note that the DA residue in produced water is in a negligible amount and should be safe even for drinking, since whole milk contains about 1300 ppm of DA [28].

Similarly, the production water flow rates for each set of test conditions were recorded for DA. Figure 5 shows the freshwater yield as a function of temperature difference from the loop. From Figure 5, the recovered water flow rate is shown to be positively related to the temperature difference. The trends shown for DA are consistent with the trends observed for OA. The freshwater yield is ~40% of the upper limit achievable from centrifuge separation. The system was able to produce desalinated water with a maximum flow rate of 28.4 ml/h at a total water/DA stream flow rate of 9000 ml/hour when the hot tank and cold tank temperature was ~67.5°C and ~47.0°C, respectively (i.e. ΔT=20.5°C).

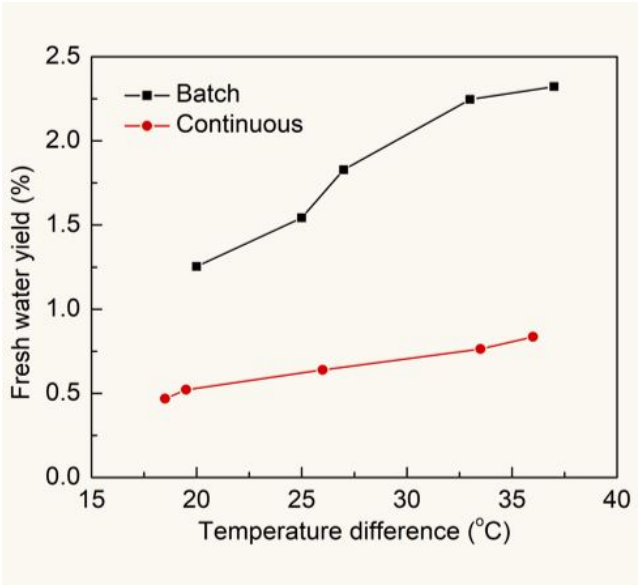

Figure 5: Freshwater yield under different ΔT from the DSE prototype using OA as the solvent, which is compared to that from a batch process with centrifuge separation.

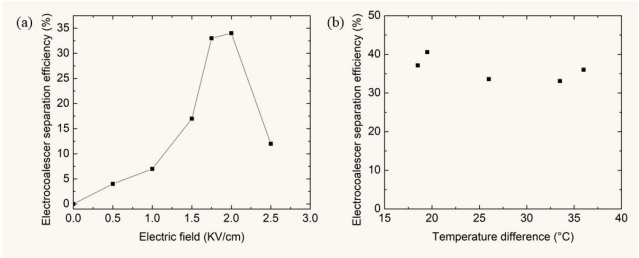

Figure 6: Freshwater yield under different ΔT from the DSE prototype using DA as the solvent, which is compared to that from a batch process with centrifuge separation.

Electro coalescer test

By comparing the freshwater yield from the continuous loop and that from the batch process, we concluded that the key factor that constrained the water yield in the continuous loop is the efficiency of the EC. The analysis of the EC efficiency is given in details as shown in Figure 6. The EC efficiency is defined as the ratio of the separated water from the EC outlet to the total separable water in the emulsion in the EC inlet, this total separable water is measured by centrifuging the emulsion enough long time so the water is 100% separated. We first studied the influence of electric field on the EC efficiency (Figure 6a). It was found that the electric field had a significant impact on the performance of the EC. In general, higher electric field leads to higher EC efficiency. A decrease was found after the electric field reached 2 kV/cm. This may be because that the EC reached its critical breakdown voltage, triggering frequent short-circuiting, which impaired the performance of the EC. We further tested the EC efficiency with emulsions obtained from different ΔT under the optimal 2 kV/cm field. As shown in Figure 6b, the efficiency was not very sensitive to temperature in the range measured, and all the calculated efficiencies were around 35%. The emulsions obtained from different temperature differences had different water droplet densities, and thus our results show that at the optimal field strength, the in-line EC efficiency is not influenced by the water content and average distance between each droplet in the emulsion in the range of interest.

The EC separation efficiency analysis reveals that the coalescer optimization is essential to increase the DSE water production. If we can double the EC separation rate from the current ~35% to ~70%, the DSE desalination production rate will also be doubled. However, despite all the successful and promising industrial applications, the principle of design and optimization for an electrocoalescer remains opaque, mainly due to the underlying complexity of the coupled physicochemical-hydrodynamic effects. Early experimental work was mainly devoted to the identification of optimum operating conditions, i.e. electric field type [31] (D.C. vs. A.C. vs. pulsed D.C.), frequency [32] (for A.C. fields), polymers for electrode coating [33], flow pattern [34], and etc. However, the understanding of the underlying mechanism remains vague, as the descriptions and explanations are not unified yet. Although they have not been thoroughly studied, the factors that determine the separation efficiency are well known to include type of applied field, field frequency, fraction of disperse phase, average inlet droplet size, surfactant, coalescer and electrode design, and etc. Among all these factors, the field strength and frequency are believed to be the most important variables to govern the electrostatic destabilization process.

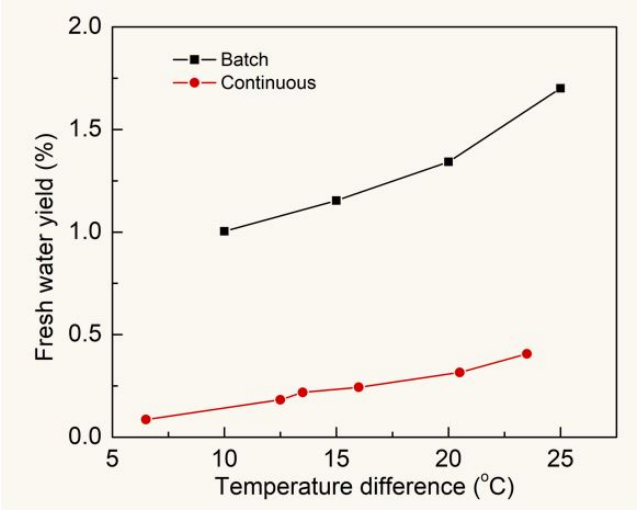

Figure 7: EC separation efficiency under different (a) electric field strengths and (b) temperatures.

To determine the optimal frequency of oscillating field and magnitude of the electric field, lots of batch experiments are conducted with various frequency and field strength. To enable the visualization of droplet coalescing under electric field, a transparent chamber (1 cm × 1 cm) and a high-speed camera was built to observe the coalescence of droplets. The chamber is made of transparent acrylic with high dielectric constant. A Nikon Eclipse Ti-E inverted optical microscope was used to observe the micro emulsion. A sCMOS camera (Hamamatsu Corporation, model C11440) is attached to the

microscope for capturing and recording the evolution of droplets during the coalescence process. The pulsed field with variable frequency is achieved by a custom-made electric circuit with four high voltage reed relays (Digi-Key Electronics) with release time 1.5 × 10-3 s to endure switching frequency up to 100 Hz. The frequency and duration time of the square oscillating field is programmed in Arduino. Figure 7 shows the emulsion evolution under electric field. Initially the micro-droplets were homogeneously distributed in space with no collective motion; the droplets lined up parallel to the field direction immediately after electric field was applied. During this stage, as larger droplets began to form, smaller nearby droplets were attracted via dipole-dipole interactions, and piecewise chains began to form along the field lines. Aggregation of piecewise chains formed intermediate large droplets, enabling the subsequent chains to be swallowed to form even larger stellar droplets; This process continued finally resulting in several large droplets.

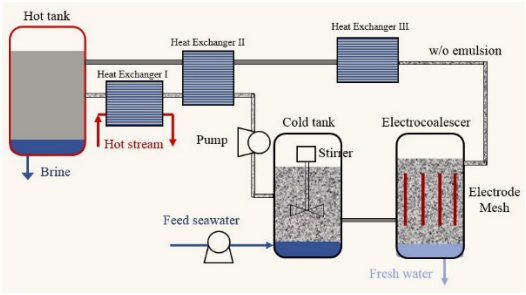

Figure 8: Electrocoalescence of water-in-oil emulsion (3.5 wt%) under 500 V/cm field intensity. (a) t=0 s; (b) t=10 s; (c) t=20 s; (d) t=30 s; (e) t=40 s; (f) t=50 s. The scale bar is 200 μm.

All the batch experiments use water-in-OA emulsions with water content 2.1 wt% and 3.5 wt%. In each set of experiments, 1 ml of emulsion was transferred to the test cell to be applied with different field intensity and frequency. The frequency values from 0.1 Hz to 10 Hz and field strength from 250 V/cm to 500 V/cm. The field strength is lower than what we used in the continuous loop, this is because we test on a much smaller sample. In all experiments, since the electrodes were not coated with a dielectric layer, short-circuiting was observed when the potential exceeded a threshold, the electric field was promptly recovered by the trip function of the power supply. From the experimental results in Figure 8, it is obvious to see that the application of an oscillating electric field assists the coalescence of micro-drops in emulsion. It is expected that differences in the mechanical and electrical relaxation times of the droplets could give rise to the existence of an optimum voltage and frequency. Emulsions have been separated with an efficiency exceeding 80% for a 60 s residence time. The process maximum efficiency (82%) was observed when the field strength was increased up to 500 V/cm, whereas an increase in field strength from 400 V/cm to 500 V/cm only resulted in unnoticeable increase in separation efficiency.

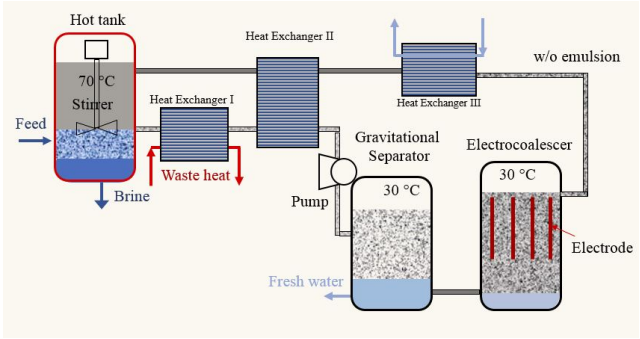

Figure 9: Water separation efficiency vs. square oscillating field frequency and field strength. (a) water content 3.5 wt%; (b) water content 2.1 wt%.

Product water quality

The exceptional ion rejection rate OA and DA and the production water quality of DSE in batch experiment has been reported elsewhere [18,20]. With gravitational separation for the emulsion separation, the DA is reported to effectively rejects at least 98% of the ions even with very high salinity water (~30 wt%). To validate the production water quality of the continuous loop, we used the inductively coupled plasma atomic emission spectra (ICP-AES) to test the water ion concentration.

Elements	Solvent-DA (ppm)	Solvent-OA (ppm)
Na	249	253
K	0	0
Ca	25	73
Mg	0	180
Fe	0	0
Cu	0	0

Table 2: ICP results of the concentrations of six metal elements in the produced water.

Economic Analysis

ICP is a powerful analytical technique used for the detection of trace elemental content in the liquid. We used ICP to determine the elemental composition of the main cations dissolved in the produced freshwater from the continuous loop. The expected cations in our samples in trace quantities included Na, Mg, K, Ca, Fe, Cu. The Fe and Cu may exist in the product water because we use stainless steel as the

electrode in the EC component. Deionized water acidified with 2% nitric acid was used as the calibration blank and for all dilutions. A total of seven standard solutions were prepared from high purity stock standards so that each metal ion would have seven calibration points. All the ICP measurements were performed on Perkin Elmer Optima 8000 equipped with WinLab 32. The water samples recovered from the DSE loop using both OA and DA were tested. The ICP results presented in Table 2 indicate that all the dissolved ions were effectively removed by the continuous DSE desalination process, and it can desalt seawater to meet the World Health Organization potable water standards (<500 ppm).

Continuous DSE process modeling with heat recovery

An economic analysis is essential to gauge the practical viability of DSE and/or to identify aspects that need further research efforts. The analysis here combines the experimental results obtained from the loop, as well as some assumptions that can be reasonably made according to the state-of-the-art industrial practice. The actual freshwater yields obtained from our lab scale loop were used for the calculations. In the lab prototype, we had no heat exchanger and used electrical heating tapes as heat sources. To estimate the required waste heat for the scaled-up plant, however, additional assumptions, e.g., heat exchanger and thermal insulation, are considered to estimate a reasonable scenario that is achievable based on the state-of-the-art engineering technologies. A system depicted in Figure 9 that can be practically designed is analyzed. As shown in the diagram, three additional heat exchangers are introduced in the loop, with Exchanger I functioning to provide solvent with the thermal energy from waste heat, Exchanger II functioning to recover the heat before the solvent being cooling, and Exchanger III functioning to cool down the solvent further to reach the lowest temperature of the loop. All the parameters related to heat exchangers in this study are assumed based on the best of our knowledge.

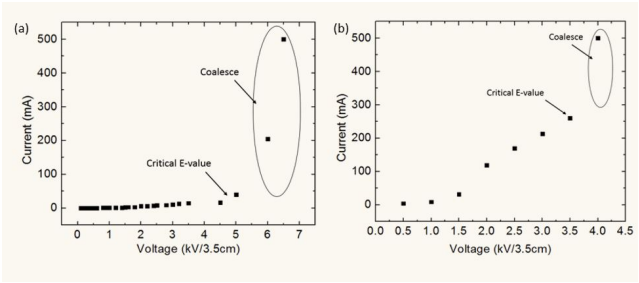

Figure 10: Diagram of a continuous DSE loop with heat recovery.

Feed Stream Mass Ratio

Energy consumption in the DSE includes both the thermal energy necessary to heat the feed solution and the electrical energy required to run the circulation pumps and electrocoalescer. Determining the mass ratio of feed water and solvent is needed for determining the amount of required DS, and eventually for determining the required thermal energy. If the ratio is too high, the DS is over-saturated, and the extra salty water remains undissolved even when heated. If the ratio is too low, the DS is under-saturated, resulting in a discount of yield performance. As the saline gets saltier by losing water molecules into DS, the affinity of water in the saline becomes stronger. There will be a balance at which water molecules can no longer escape from the saline to diffuse into DS. The perfect mixing ratio would allow the solvent to be saturated during the mixing process at the high-temperature tank, while the un-dissolved salty water reaches a salinity that does not allow more water molecules to diffuse from the saline to DS. This balance, however, has not yet been accurately measured, and it is out of the scope of this study. However, a previous study has shown that DA and OA can still extract water from saline even when the salinity is 10% [20]. The upper limit is likely higher, but we chose to use this known number of 10% to guarantee the validity of the following calculations. To determine the amount of feed water for producing 1 unit of freshwater, we assume the concentrated brine water reaches a salinity of 10% when it is disposed. If y is the amount of feed water, we have the mass of salt ions conserved as:

$$y \times 3.5\% = (y-1) \times 10\% \quad (1)$$

In this case, to produce 1 unit of water from a saline source with a salinity of 3.5% (seawater), the amount of feed saline water is 1.54 units, leading to a ~65% water recovery rate.

The temperature dependency of freshwater yield from our continuous prototype was obtained in Figures 4 and 5. The extracted slope in Figure 4 shows that using OA as the solvent, 0.78% of freshwater yield can be obtained when the temperature difference is 40C. The amount of OA that needs to be cycled to obtain 1 unit of freshwater with a temperature difference of 40C is thus 1/0.78%=128.21 units. The total mixture volume is then 129.75 units. Similarly, the extracted slope in Figure 5 shows that 0.72% of freshwater yield can be achieved when using DA as the DS. The amount of DA that needs to be cycled is then 1/0.72%=138.89 units. The total mixture volume is then 140.43 unit. As we can see, the feed stream is dominantly DS, and thus most of the fluid in the stream would then be DS. As a result, it is assumed that the properties of the fluid are the same as those of DS, which will not lead to any significant error in calculation.

Required thermal energy

We note that heat exchangers can be implemented to recover heat from the hot stream to warm up the cold stream. Modeling work specifically studying heat recovery for the DSE system has been previously done [21]. Since heat exchangers are mature technologies and their applications are still subject to engineering optimization for the DSE desalination, we choose not to test them in this first demonstration of a continuous DSE loop, but simply assume the state-of-the-art heat exchanger thermal recovery efficiencies in the thermodynamic calculations.

The thermal energy transport from waste heat to the DS can be realized by the heat exchanger (Exchanger I) as in Figure 9. The thermal energy estimation is necessary to determine the required heat exchanger area and pump power. In a real DSE plant, a heat exchanger (Exchanger II, Figure 9) can be incorporated between the hot and cold streams to minimize the amount of external heat needed by the system. Although our lab scale loop did not test heat exchanger, the state-of-the-art heat exchangers can have efficiencies routinely over 80%, meaning that only 20% of the total energy required to heat up the feed stream is needed from the waste heat [35]. We set T_H to be the highest temperature of the mixture and T_L to be the lowest temperature at which water precipitation occurs. If we ignore the heat loss in the pipelines and devices to the environment, which can be

realized using good thermal insulation materials, then the required waste heat to heat up the mixture is:

$$Q = mC_p(T_H - T_L) \times 20\% \qquad (2)$$

where m is the mass of the solution, C_p is the specific heat capacity of the fluid.

Required electrical energy for EC

EC is generally considered the most energy efficient technique compared to other phase separation methods, such as filtration and centrifugation [24]. However, there is no valid theory that can accurately predict the power consumption of the coalescer, since it is influenced by many factors like the voltage, oscillating frequency, waveform of the applied electric field, electrode geometry and configuration, agitation speed of mixing, and the physical-chemical properties of the emulsion [24,36]. In this study, for example, the principal parameters needing examination are electrical voltage, current, and electrical conductivity of the emulsion to determine the power consumption. The conductivity of pure water, pure fatty acid, and water-in-OA emulsion is measured to be 47 μs/cm, 0 μs/cm, 0 μs/cm, respectively using a conductivity meter. The electric resistance characteristic of the emulsion under high voltage, however, is dynamic and can increase drastically if water chains are developed to bridge the electrodes. In this study, we only have a proof-of-concept first design of the electrocoalescer to show that it can work. The energy consumption of coalescence is hard to determine at this stage because the water-in-DS emulsion is volatile, and the consumed power is not steady, not to mention occasional short-circuiting. The EC design definitely requires intensive research, where the efficiency and the energy consumption need to be optimized.

Lee et al. reported that the electrical energy consumption under alternative-current field was measured to be between 0.053 and 0.528 kWh/m^3 emulsion, while that for pulsed direct-current was measured to be between 0.056 and 0.695 kWh/m^3 emulsion [37]. In their study, the treated emulsion was water-in-Isopar M emulsion with the water content of ~20 wt%, and the estimated electricity costs for an industrial-scale electrical demulsifier were reported to be as low as $0.37 per 1000 oil barrels, which is equivalent to 0.23 cents per cubic meter emulsion. NATCO also reported comparable costs of as low as $0.23 per 1000 barrel for an industrial-scale electrocoalescer [38]. However, both values were obtained from crude oil systems consisting of nearly 20% water. Since water content only counts less than 3.5 wt% of our water-in-DS emulsion, lower power consumption is expected since the emulsion is less electrically conductive.

Required electrical energy for pumping and heat exchanger capital cost

If we assume the pipe to be ideally smooth and there is no gravitational potential difference, the energy required to pump the salt water, DS and water/DS mixture in the system is negligible, then most of the pressure drop in the entire DSE system is due to the friction of surface wall in the heat exchanger. The required heat exchanger area and the pressure loss in the heat exchanger have been estimated in previous studies [21,22]. Alotaibi et al. estimated that the electrical energy consumption for pumping is around 10 kWh/m^3 of produced freshwater when using DA as the solvent [21]. With the assumption that the hydraulic diameter of heat exchanger conduits is 0.05 m and the driving force for heat transfer across the heat exchanger surfaces is 5 K, the consumed power density for pumping using OA as the solvent is estimated to be 7.44 kWh/m^3 of produced freshwater [22].

Economic analysis

The major cost elements for desalination plants are capital costs and operational costs. Capital costs include procurement cost of land, material, and equipment to build the new plant, labor charges, as well as cost of permits and licenses to build the plant. Operational costs include labor, materials, required thermal and electrical energy cost, pre-treatment, maintenance cost, environmental impact cost, consumables, etc., as well as licenses, permits, and certifications required to run the plant. It is worthy emphasizing that this economic analysis is just a rough order of magnitude calculation to identify future research needs. In this analysis, we are not including the costs for land, construction of the plant, and labor for operation and maintenance, since these are standard economic analyses that can be found from the local market perspective and only add limited cost to the overall cost. We have also excluded the cost of permits, licenses or certifications from this analysis. The capital cost of the heat exchanger is $24,000 per cubic meter per day capacity [22]. If we assume a 30-year depreciation time, the capital cost is estimated to be $2.19/m^3 of freshwater. The assumptions for the economic analysis are summarized as:

- DS can extract water from saline when the salinity is 10%, leading to a ~65% water recovery;
- The electricity cost for EC is assumed to be 0.23 cents per cubic meter emulsion;
- The electricity consumption for pumping is assumed to be 10 kWh/m^3 of freshwater for DA and 7.44 kWh/m^3 of freshwater for OA.

The U.S. Energy Information Administration has statistics on the industrial average price of electricity to be 7.18 cents/kWh in September 2015 [39]. For producing 1 m^3 freshwater using OA as the solvent, the cost breakdown is given in Table 3. To produce 1 m^3 of freshwater the cost would be $3.03 in total.

Cost Breakdown	Quantity	Unit Price	Costs (cent)
Electrocoalescer	129.75 m^3	0.233 cent/m^3	30.23
Pump	7.44 kWh	7.18 cents/kWh	53.42
Heat exchanger	1 m^3	$2.19/m^3	219.18

Total	302.83

Table 3: The breakdown of the costs to produce 1 m^3 freshwater using OA as the solvent.

There are still places that we can optimize and improve to reduce the energy requirement and cut down costs.

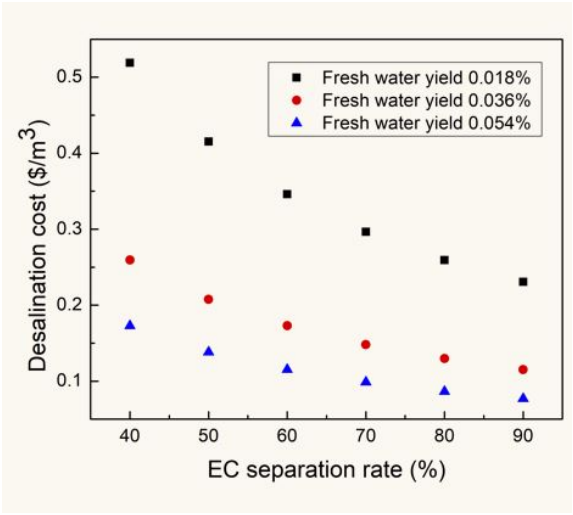

Figure 11: DSE desalination costs with better EC separation efficiency and DS with higher freshwater yield.

For example, EC separation in the prototype can only reach up to 40%, while some commercial electrostatic dehydrators are reported to have efficiencies as high as 90% [40-42]. The costs of DSE desalination will drastically decrease with a better EC separator. The overall cost can also be reduced if we can find DS with better freshwater yield. As shown in Figure 10, we plot the DSE desalination cost as a function of EC separation efficiency and DS with different freshwater yields (%/C). If we can achieve a four-fold increase in DS effectiveness over the currently used DS and an EC efficiency of 90%, DSE may lead to an operational cost less than \$0.25/m^3. Furthermore, capital cost from the heat exchanger contributes the majority of the total cost. We note that we can potentially use plastic heat exchangers instead of metallic ones since the DSE desalination operates at relatively low temperatures (<70C) and the temperature difference between the streams are not very significant. This would drastically reduce the capital cost.

It is worth noting here that we have not considered the costs of waste heat in our economic analysis. Although waste heat itself can be free, access to waste heat from power plants may cost money. However, this should not be a major cost. Achievable costs of desalinating seawater using conventional technologies range from \$0.45 to \$1.00/m^3 in large plants [17]. However, more than half of the total cost of desalination comes directly from energy cost. Since energy price is destined to increase with the depletion of fossil energy, it is important to explore more desalination technologies using alternative energy as input. Comparing the costs of DSE desalination, it is apparent that DSE can be competitive economically if we tackle the technical barriers outlined above.

Conclusion

In this work, a lab-scale continuous DSE prototype with the capacity of producing 28 ml/h freshwater was presented. The freshwater yield of the DSE prototype under different conditions was also analyzed. The EC efficiency was measured to be 35% for OA and 20% for DA and is the bottleneck for the water productivity. Certain potential design improvements (e.g., implement of the heat exchanger) to increase the efficiency and decrease the energy consumption and cost are also discussed. The results reveal that further research is needed to (1) identify more efficient DS with higher freshwater yield; (2) optimize the EC design to reduce the electrical energy costs.

In summary, the current work lays a framework upon which further research on the continuous DSE desalination process can be based. The preliminary cost analysis shows that the coupling of renewable/waste energy and the DSE desalination process is promising and worth further exploration.

Acknowledgments

This research is partially supported by National Science Foundation (award #: 1510826, program officer: Dr. William Copper) and the Electrical Power Research Institute (managed by Dr. Gabriel Ilevbare). The ICP and DLS analyses were conducted at the Center for Environmental Science and Technology (CEST) at the University of Notre Dame. T.L. would also like to thank the Dorini Family for the endowed professorship in energy studies.

References

1. Hoffmann S (2009) Planet Water: Investing in the World's Most Valuable Resource. John Wiley & Sons.
2. Elimelech M, Phillip WA (2011) The future of seawater desalination: energy, technology, and the environment. Science 333: 712-717.
3. Nikolay V (2016) Desalination-Past, Present and Future.
4. Zhou Y, Tol NV (2005) Evaluating the costs of desalination and water transport. Water Resour Res, p: 41.
5. Veerapaneni S, Long B, Freeman S, Bond R (2007) Reducing energy consumption for seawater desalination. JournalAmerican Water Works Association 99: 95-106.
6. Service RF (2006) Desalination freshens up. Science 313: 1088-1090.
7. Shannon MA, Bohn PW, Elimelech M, Georgiadis JG, Marinas BJ, et al. (2008) Science and technology for water purification in the coming decades. Nature 452: 301-310.
8. Yang J, Pang Y, Huang W, Shaw SK, Schiffbauer J, et al. (2017) Functionalized graphene enables highly efficient solar thermal steam generation. ACS Nano 11: 5510-5518.
9. Wangnick K (2002) IDA worldwide desalting plants inventory. Produced by Wangnick Consulting for the International Desalination Association, Gnarrenburg, Germany, p: 10.
10. Fritzmann C, Löwenberg J, Wintgens T, Melin T (2007) State-of-the-art of reverse osmosis desalination. Desalination 216: 1-76.
11. Peng G, Ding H, Sharshir SW, Li X, Liu H, et al. (2018) Low-cost high-efficiency solar steam generator by combining thin film evaporation and heat localization: Both experimental and theoretical study. Applied Thermal Engineering 143: 1079-1084.

12. Sharshir SW, Peng G, Elsheikh AH, Edreis EM, Eltawil MA, et al. (2018) Energy and exergy analysis of solar stills with micro/nano particles: A comparative study. Energy Conversion and Management 177: 363-375.
13. Sharshir SW, Peng G, Wu L, Yang N, Essa FA, et al. (2017) Enhancing the solar still performance using nanofluids and glass cover cooling: experimental study. Applied Thermal Engineering 113: 684-693.
14. Fang Z, Zhen YR, Neumann O, Polman A, García de Abajo FJ, et al. (2013) Evolution of light-induced vapor generation at a liquid-immersed metallic nanoparticle. Nano Letters 13: 1736-1742.
15. Greenlee LF, Lawler DF, Freeman BD, Marrot B, Moulin P (2009) Reverse osmosis desalination: water sources, technology, and today's challenges. Water Research 43: 2317-2348.
16. Marks DH, Balaban M, Falagan BA, Jacangelo JG, Jones KL, et al. (2004) Review of the desalination and water purification technology roadmap. National Research Council, National Academies Press, Washington, DC.
17. Karagiannis IC, Soldatos PG (2008) Water desalination cost literature: review and assessment. Desalination 223: 448-456.
18. Bajpayee A, Luo T, Muto A, Chen G (2011) Very low temperature membrane-free desalination by directional solvent extraction. Energy and Environmental Science 4: 1672-1675.
19. Luo T, Bajpayee A, Chen G (2011) Directional solvent for membrane-free water desalination-A molecular level study. Journal of Applied Physics, p: 054905.
20. Rish D, Luo S, Kurtz B, Luo T (2014) Exceptional ion rejection ability of directional solvent for non-membrane desalination. Applied Physics Letters, p: 024102.
21. Alotaibi S, Ibrahim OM, Luo S, Luo T (2017) Modeling of a continuous water desalination process using directional solvent extraction. Desalination 420: 114-124.
22. Sanap DB, Kadam KD, Narayan M, Kasthurirangan S, Nemade PR, et al. (2015) Analysis of saline water desalination by directed solvent extraction using octanoic acid. Desalination 357: 150-162.
23. Bajpayee A (2012) Directional solvent extraction desalination. Doctoral dissertation, Massachusetts Institute of Technology.
24. Eow JS, Ghadiri M, Sharif AO, Williams TJ (2001) Electrostatic enhancement of coalescence of water droplets in oil: a review of the current understanding. Chemical Engineering Journal 84: 173-192.
25. Kokal SL (2005) Crude oil emulsions: A state-of-the-art review. SPE Production and Facilities 20: 5-13.
26. Noïk C, Chen J, Dalmazzone CS (2006) Electrostatic demulsification on crude oil: A state-of-the-art review. In International Oil & Gas Conference and Exhibition in China. Society of Petroleum Engineers.
27. Luo S, Schiffbauer J, Luo T (2016) Effect of electric field non-uniformity on droplets coalescence. Physical Chemistry Chemical Physics 18: 29786-29796.
28. Pešek M, Špička J, Samková E (2005) Comparison of fatty acid composition in milk fat of Czech Pied cattle and Holstein cattle. Czech J Anim Sci 50: 122-128.
29. Luo S, Schiffbauer J, Luo T (2017) Effect of cooling on droplet size in supersaturation-induced emulsions. Physical Chemistry Chemical Physics 19: 29855-29861.
30. Windholz M, Budavari S, Blumetti R, Otterbein E (1983) An encyclopedia of chemicals, drugs, and biologicals. The Merck Index, 10th edn. Merck and Co Inc, Rahaway, New Jeresy, USA.
31. Mousavichoubeh M, Ghadiri M, Shariaty-Niassar M (2011) Electro-coalescence of an aqueous droplet at an oil-water interface. Chemical Engineering and Processing: Process Intensification 50: 338-344.
32. Zagnoni M, Cooper JM (2009) On-chip electrocoalescence of microdroplets as a function of voltage, frequency and droplet size. Lab on a Chip 9: 2652-2658.
33. Fjeldly TA, Hansen EB, Nilsen PJ (2006) Novel Coalescer Technology in First-Stage Separator Enables One-Stage Separation and Heavy-Oil Separation. Offshore Technology Conference.
34. Melheim JA, Chiesa M (2006) Simulation of turbulent electrocoalescence. Chemical Engineering Science 61: 4540-4549.
35. Fakheri A (2014) Efficiency analysis of heat exchangers and heat exchanger networks. International Journal of Heat and Mass Transfer 76: 99-104.
36. Eow JS, Ghadiri M (2002) Electrostatic enhancement of coalescence of water droplets in oil: a review of the technology. Chemical Engineering Journal 85: 357-368.
37. Lee CM, Sams GW, Wagner JP (2001) Power consumption measurements for ac and pulsed dc for electrostatic coalescence of water-in-oil emulsions. Journal of Electrostatics 53: 1-24.
38. Suemar P, Fonseca EF, Coutinho RC, Machado F, Fontes R, et al. (2012) Quantitative evaluation of the efficiency of water-in-crude-oil emulsion dehydration by electrocoalescence in pilot-plant and full-scale units. Industrial & Engineering Chemistry Research 51: 13423-13437.
39. US Energy Information Administration (2015) Electric Power Monthly with Data for December 2015.
40. Lesaint C, Berg G, Lundgaard L, Ese MH (2016) A novel bench size model coalescer: dehydration efficiency of AC fields on water-in-crude-oil emulsions. IEEE Transactions on Dielectrics and Electrical Insulation 23: 1-6.
41. Lesaint C, Glomm WR, Lundgaard LE, Sjöblom J (2009) Dehydration efficiency of AC electrical fields on water-in-model-oil emulsions. Colloids and Surfaces A: Physicochemical and Engineering Aspects 352: 63-69.
42. Less S, Vilagines R (2012) The electrocoalescers' technology: Advances, strengths and limitations for crude oil separation. Journal of Petroleum Science and Engineering 81: 57-63.